Materials for Renewable and Sustainable Energy (2022) 11:1–15
https://doi.org/10.1007/s40243-021-00203-y

ORIGINAL PAPER

Passive solar house prototype design with a new bio-based material for a semi-arid climate

Cherif Boulebbina[1] · Ghazali Mebarki[1] · Samir Rahal[1]

Received: 2 June 2021 / Accepted: 26 November 2021 / Published online: 21 December 2021

Abstract

In this study, a passive solar house prototype was built using Trombe wall and was tested in the semi-arid region of Batna, in eastern Algeria. Traditional local materials (stone and adobe) were used for the construction of the thermal storage wall. A new local bio-based material made from date palm trunks was used for the insulation of the passive house prototype. For a better understanding of passive house heating and for a comparative study, a numerical simulation, using Fluent, was carried out. The aim of this study was to supply recommendations for improving the passive systems and to participate to the energy consumption control in the building sector. The results show that the experimental and numerical simulation results are in good agreement. The optimal orientation of the solar passive house has been determined, which is at 160° southeast. The use of local and bio-based materials has proven its effectiveness in the construction of the passive house. The thermal behavior of date palm wood has been found to be close to those of insulation materials commonly used in buildings. That means it has the same thermal insulation ability (thermal conductivity). On the other hand, the results show that the thermal efficiency of the passive solar heating system, with an adobe wall is significantly higher (50%) than that with a stone wall (30.7%).

Keywords Passive heating · Semi-arid region · Bio-based materials · Energy efficiency · Trombe wall · Adobe

List of symbols

G	Global solar radiation flux density (W/m^2)
A	Surface (m^2)
H	Height (m)
T	Temperature (°C)
V	Fluid velocity (m/s)
m	Air mass flow rate (kg/s)
a	Thermal diffusivity (m^2/s)
Cp	Specific heat (J/kg°C)
g	Acceleration of gravity (m/s^2)
t	Time (s)
e	Thickness (m)
Q	Heating capacity (W)
R	Thermal resistance (m^2.°C/W)
hc	Convection coefficient (W/m^2°C)
hr	Radiation coefficient (W/m^2°C)
Ra	Rayleigh number
Gr	Grashof number
Nu	Nusselt number
Pr	Prandtl number
X	Independent variable of equations

Greek letters

ρ	Density (kg/m^3)
μ	Dynamic viscosity (kg/ms)
ν	Kinematic viscosity (m^2/s)
β	Thermal expansion coefficient (°C^{-1})
λ	Thermal conductivity (W/m^2°C)
α	Solar absorptivity
ε	Emissivity
τ	Transmissivity
σ	Stefan Boltzmann constant (5.67×10^{-8} W/m^2°K^4)
ϕ	Heat flux (W)
η	Average thermal efficiency (%)

Subscripts

c	Channel
w	Wall
g	Glazing
cond	Conduction
conv	Convection
amb	Ambiance
i	Interior
e	Exterior

✉ Ghazali Mebarki
g.mebarki@univ-batna2.dz

[1] LESEI Laboratory, Mechanical Engineering Department, Faculty of Technology, University of Batna 2, Avenue Chahid Boukhlouf Mohammed Elhadi 05001, Batna, Algeria

f	Fluid
r	Radiation
tv	Top vent
bv	Bottom vent
out	Outside
exp	Experimental
sim	Simulation

Introduction

Because of the increase in the energy requirements in buildings, solar energy becomes the most suitable solution due to its free availability. The popularity of passive solar energy systems has increased massively and Trombe wall system becomes a very interesting heating technique in buildings. The passive solar heating is widely used in cold climates, especially by Trombe wall system also named thermal storage wall [1]. It is a massive wall which is painted with a dark color to absorb the maximum amount of heat from incident solar radiation. The storage wall is covered with glass from outside and an insulating air-gap between them. The Trombe wall is a passive solar building design strategy that adopts the concept of indirect-gain, where the solar radiation absorbed by the wall is converted to heat and then transferred into the internal space of the building by radiation, conduction and natural convection through vents (orifices) at the bottom and top of the wall [2, 3]. Many studies have been conducted on the passive heating by the Trombe wall system [4]. An experimental and numerical study was conducted by Liu et al.[5] on a passive house prototype. Analysis of thermal performance parameters of the Trombe wall provided the optimal opening and closing modes in the management of air vents. The results provided a reference base for optimizing the design of a passive solar house with Trombe wall. Briga-Sá et al. [6], experimentally, analyzed a test cell with a classical Trombe wall submitted to real climatic conditions in a Portuguese city. They found that ventilation openings and shading affect the temperatures fluctuation and, therefore, the system ability to store and release heat. The paper of Bajc et al. [7] deals with a comprehensive numerical CFD analysis of temperature fields in Trombe wall for a moderate continental climate using different types of glassing on the outside of the wall. Depending on these results, analysis of energy savings potential is performed. Experiments of Dong et al. [8], using a novel designed Trombe wall, proved that daily thermal efficiency on the heating performance is able to heat the indoor space effectively and rapidly and is higher than 50% during the daytime. A numerical and experimental results, by comparing heating performances of several new designed systems during winter period which are provided by K. Hami et al. [9], showed that it is able to keep the room warm sufficiently and meets the standards of air conditioning. That aim can be reached by diminishing the implementation costs of the Trombe wall to provide a comfortable indoor temperature. The Trombe wall is able to keep the room warm enough along with decreasing the implementation costs of the Trombe wall and occupying less space. The area of the Trombe wall is equal to 50% of that of the southern wall [10]. Three zones have been tested in Algerian climatic conditions by setting up of passive heating systems developed by Imessad [11]. Through this study, they found that the system reduces the annual heating needs by 60–70%. Additionally, they proved that optimization of solar system depending on the Life Cycle Cost (LCC) criterion by S. Jaber et al. [12] can lead to develop an approach for optimum size designing the most economic residential building in the mediterranean region. Their study provides also many advantages such as the reduction of LCC by 2.4%, the area ratio from thermal and economical point of view being 37%. Furthermore, about 445 kg of CO_2 are reduced annually. Abbassi et al.[13] carried out a study of energy performance of a Trombe wall prototype system on the Mediterranean coast. They showed that high thermal inertia walls and thermal insulated walls can greatly decrease the heating needs. They show that a Trombe wall with 4 m^2 area can save up to 50% of auxiliary heating energy per year and 77% can be saved with a Trombe wall with an area of 8 m^2. A 63% energy reduction can be achieved by a Trombe wall with 3 m^2 area if the building walls are insulated. A fair agreement between analytical and numerical results was obtained by the model proposed by Abdeen et al. [14] combined with experimental validation of optimal design model Trombe wall. The thermal comfort was improved by 38.19% under typical winter week. A Trombe wall performance for a room located in Yazd (Iran) was studied numerically by Rabani et al. [15]. The results showed that the Trombe wall made of paraffin wax can keep the room warmer in comparison with other materials for about 9 h. A new Trombe wall design which guarantees the maximum hourly stored energy (about 1600 kJ/h more than a normal system) was realized under Yazd (Iran) desert climate by Rabani et al. [16]. The new designed Trombe wall improves the average daily heating efficiency by about 27%. Mohamad et al. [17] proposed a novel design for heating and ventilating rooms using solar energy in the winter season and for reducing the cooling load in the summer season. The system utilizes a water tank, which is part of the building's wall, for storage and hot water supply. The results showed that the proposed system is more thermally efficient as compared to the conventional Trombe walls. Hassanain et al. [18] investigated the following three different greenhouse prototype designs: gable, flat and semi-circle roof shapes at Suez-Canal University (Egypt). The effect of using the adobe wall, as solar heat storage, was studied. A range of inexpensive and available materials were used to form the adobe wall. It is found that, the flat shape greenhouse surface gives higher air temperatures when the direction of the greenhouse was north–south. An innovative Trombe wall with an extra window in the massive wall is suggested by Bellos et al. [19] and compared with the conventional Trombe wall and the usual insulated wall. The examined building is located in Athens, Greece. According to the results, the new Trombe wall is the most appropriate technology, creating warmer indoor profile than the other cases. Bevilacqua et al. [20] proposed the use of proper ventilation strategies to reduce cooling needs. The effectiveness verified in warm climates, where the Trombe wall reduced the heating needs by 71.7% and the demand for cooling energy by 36.1%. However, in a cold climate, heating savings were 18.2% with a cooling energy reduction of 42.4%. A numerical study proposed by Błotny et al. [21] considered passive solar heating and cooling system in Poland. In order to examine the temperature distribution and air circulation in a room for two representative days during heating and cooling periods. A temperature increase of 1.11 ◦C and a temperature decrease in the morning and afternoon of 2.27 °C were obtained. Furthermore, the results obtained by changing the wall material from concrete to brick showed a temperature increase of 0.40 °C near the storage layer. An innovative Trombe wall configuration designed for cold climates, named a thermo-diode Trombe wall, was used by Szyszka et al. [22], to improve the energy efficiency by providing a proper level of insulation for the building envelope. The results showed that in presence of solar radiation, the thermo-diode Trombe wall was able to generate significant heat transfer by natural convection inside the air cavity, with temperatures higher than 35 °C in the upper section. The efficiency, relative to the incident solar radiation, reached 15.3% during a well-sunny winter day.

Using the Trombe wall in the building can reduce energy consumption and heating demand, in addition to being environmentally friendly. It is clear that the Trombe wall improves the energy efficiency and sustainability of buildings by using bio-based insulation materials. Indeed, an important development of thermal insulation over the years is observed, particularly during the second half of the twentieth century and the beginning of this century [23, 24]. The implementation of the Algerian National Energy Efficiency Program 2030 [25] through a variety of actions and projects promotes the emergence of a sustainable energy efficiency market in Algeria [26]. The objective of this program was to encourage innovative practices and technologies for improving the interior comfort of the dwellings, and using less energy, also preserving the environment. This can be done from the concept of sustainable development and bio-evolution based on the building blocks made of materials from renewable biological resources. Many in-depth studies have been devoted to new materials derived from biological sources or traditional composite materials in order to meet the requirements of the appropriate thermo-physical properties [27]. In order to achieve perfect insulation and introduce the concept of "sustainability" to contribute significantly to the energy efficiency, investigators are currently seeking to develop thermal and acoustic insulation materials, using natural or recycled materials for their application because their performance is similar to others synthetic materials [28, 29].

Algeria is a large country with more than 18.6 million date palms cultivated on an area of 169,380 hectares [30]. However, significant residues of palm trees or dry palm trunks are generated and then lead to a pollution of the environment when burned. Plant waste, like palm wood, has been used for the production of multi-layered wood panels by several searches [28, 29]. Many innovative techniques use the different parts of the date palm mixed with different basic building materials to produce bio-based materials [31–35].

In this study, a sustainable building approach was adopted in semi-arid climatic conditions of Batna (Algeria), in order to use efficiently the solar energy. For that purpose, this study contributes to the control of energy consumption and thermal comfort in the housing sector. The thermal behavior of passive solar heating is examined through a passive solar house prototype during typical winter days. The thermal storage wall of the Trombe wall was built with traditional local materials, Adobe and stones which are widely used in old buildings. A new local bio-based (bio-sourced) material was used, that is made of trunks of date palms, for the insulation of the sidewalls of the passive house. Solar thermal efficiency was calculated for different facade materials and different orientations in order to identify the optimal orientation and best material to use for best passive solar heating. In addition, numerical simulation was carried out in order to further illustrate the parameters of flow and heat transfer in the passive solar heating system.

Experimental set up and procedure

Passive house design

A passive house prototype was designed and tested at the University of Batna 2 located at the city center of Batna in the east of Algeria (Fig. 1), which is a semi-arid climates region. In winter, temperatures can drop below freezing at night and reach 45 °C in the shade during summer. To provide thermal comfort and energy saving, Trombe wall (also named thermal storage wall) is used.

Solar radiation is absorbed by the storage wall and thus converted into thermal energy and transferred into the internal space of the house (Fig. 2).

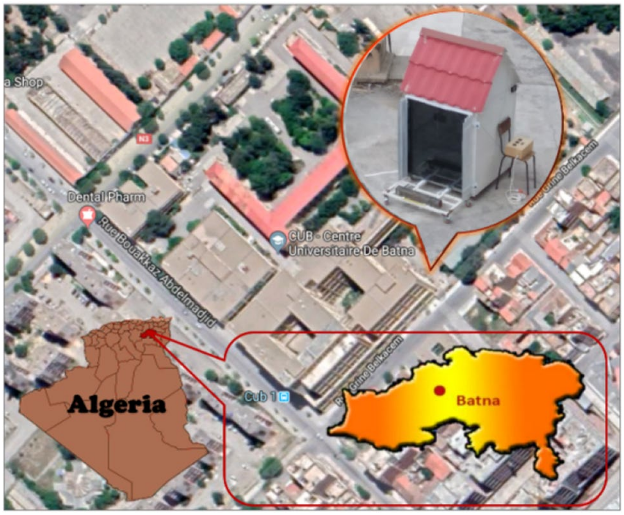

Fig. 1 Passive house prototype experimental site

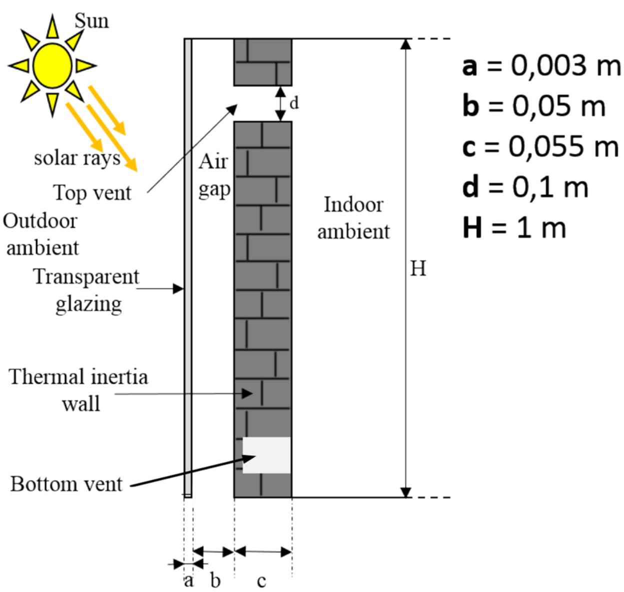

Fig. 2 Thermal storage wall

The passive house has a parallelepiped shape with an interior volume of 1 m^3 (Fig. 3a). For better thermal insulation, the roof and the floor are made of two layers, a layer of wood and a layer of expanded polystyrene. To be moved freely and easily during experimental tests, the prototype is equipped with wheels at its base as shown in Fig. 3b. The passive house prototype walls (except the storage wall) are made of multilayer materials with an intermediate layer of insulating material having a thickness of 4.6 cm (Fig. 3c).

For the thermal insulation of the prototype, a locally produced bio-based material was used for the two sidewalls while for the back side, expanded polystyrene was chosen. The bio-based material was made from date palm wood (Fig. 4). In Algeria, thousands of date palms are burned every year inducing pollution. Such date palms can be recycled and used as materials for insulating buildings.

The thermal storage wall is removable to allow testing of several types of materials. For that purpose, two different materials were used: natural stones from the Aurès Mountains (east of Algeria) (Fig. 5a) and Adobe (sun-dried bricks made from a mixture of 70% clay, 20% straw and 10% water) (Fig. 5b).

Experimental measurements

The measurements were carried out on the prototype of the passive house for typical winter days in the city of Batna. The following three orientations of the passive house were examined: 160° South-east, 180° South and 200° South-west (Fig. 6a). Surface and ambient temperatures were measured every 15 min from 10:00 to 17:00. Internal surface temperatures (T_i) were measured using K thermocouples located on the four interior surfaces centres. These thermocouples are connected to a 176 T4 data logger (Fig. 6b) which exports the measurement results to a computer by means of an USB connection. Other thermocouples are used to measure indoor air temperatures (T_{in}), outdoor air temperatures (T_{ex}) and air gap temperatures (T_c) between the glazing and thermal storage wall. Measured values are displayed on a digital screen (Fig. 6c). The temperatures of the exterior surface

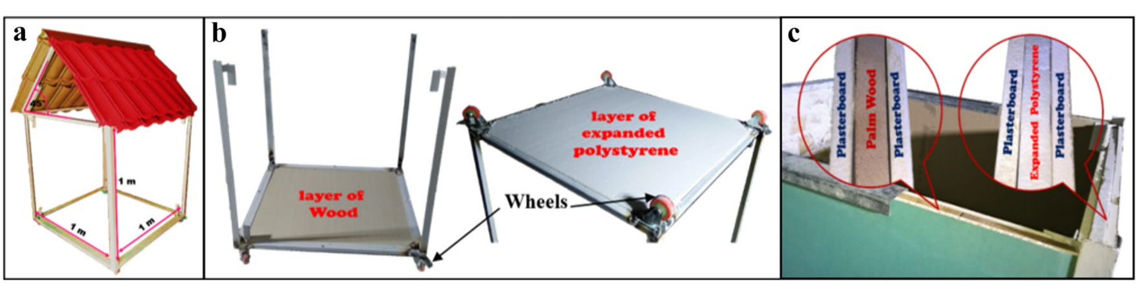

Fig. 3 **a** Basic structure of the prototype, **b** Floor insulation, **c** Multilayer insulating walls

Fig. 4 Preparation of bio-based material

Fig. 5 Thermal storage wall materials **a** Stones facade, **b** Adobe facade

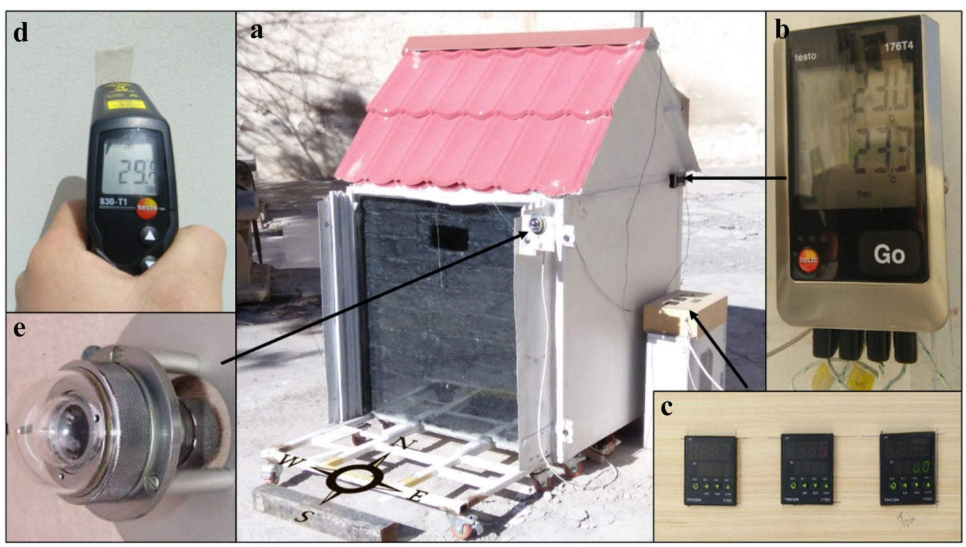

Fig. 6 Experimental measuring devices

of the house (T_e) are measured using an infrared sensor (Testo 830-T1) (Fig. 6d). The solar radiation flux density is measured by Kipp & Zonen CM 5/6 Pyranometer fixed on the facade of the passive house (Fig. 6e). Finally, wind speed and relative humidity data are obtained using a weather station.

Modelling and numerical simulation procedure

Mathematical modelling

In this study, a heat transfer analysis of the different parts of the passive solar house prototype was performed. In this passive solar-heating system, solar radiation is absorbed by the external face of the thermal storage wall; then heat is transferred inside the passive house by conduction through the storage wall, by radiation and natural convection.

The solar radiation that goes through the glass and then absorbed by the thermal storage wall, is given as follows:

$$\Phi = \tau_g \alpha_w G, \tag{1}$$

where τ_g is the glass transmittance, α_w is the wall absorptivity and G is the solar radiation.

Combined heat flux density between the outer face of the glass and the ambient outside air by convection and radiation [36] as follows:

$$\Phi_{out} = h_{ce}(T_{amb} - T_g) + h_{re}(T_{sky} - T_g), \tag{2}$$

where T_{amb} and T_g are the ambient and glass temperatures, respectively.

Convective heat transfer coefficient h_{ce} is given as follows [37]:

$$h_{ce} = 5.7 + 3.8\mathrm{V}_{wind} \tag{3}$$

Radiation heat transfer coefficient h_r is given as follows [37]:

$$h_{re} = \sigma\varepsilon_g(T_{sky}^2 + T_g^2)(T_{sky} + T_g), \tag{4}$$

where ε_g is the emissivity of glass and σ is Stefan–Boltzmann constant ($\sigma = 5.67 \times 10^{-8}\ \mathrm{W/m^2\ K^4}$). Sky temperature T_{sky} is given by Swinbank [14] as follows:

$$T_{sky} = 0.0552\, T_{amb}^{1.5} \tag{5}$$

Average convective heat transfer coefficient in the air-gap between the thermal storage wall and the glass is given by [38]:

$$h_{cc} = 5.68 + 4.1V_{air} \tag{6}$$

The mass flow rate in the air-gap is calculated by:

$$\dot{m} = \rho V_{air} A_c, \tag{7}$$

where ρ is the air density and A_c is the air-gap area.

V_{air} is the mean air velocity in the air-gap, determined by [13] as follows:

$$\mathrm{V}_{air} = \left[\frac{2gH \cdot (T_c - T_i)}{(C_1(A_c/A_v)^2 + C_2) \cdot T_c}\right], \tag{8}$$

where T_c is the mean air temperature in the canal, T_i is the inside (room) air temperature, H is the wall height, A_v is the vent area and g is the gravitational acceleration.

$C_1 = 8$ and $C_2 = 2$ are empirical constants determined by Utzinger [13].

The energy transmitted to the inside of the passive house via the top vent is given by [39] as follows:

$$Q_{conv} = \frac{\dot{m}Cp\,(T_{tv} - T_{bv})}{A_w}, \tag{9}$$

where T_{tv} is the top vent temperature, T_{bv} is the bottom vent temperature, Cp is the specific heat of air and A_w is the wall area (m^2).

The Nusselt number in the air-gap is determined according to the correlations proposed by Curchill and Chu [36] as follows:

For laminar free convection ($Ra_H < 10^9$):

$$\mathrm{Nu} = 0.68 + \frac{0.67\,(\mathrm{Ra_H})^{1/4}}{\left[1 + (0.492/\mathrm{Pr})^{9/16}\right]^{4/9}} \tag{10}$$

For turbulent free convection ($Ra_H > 10^9\sqrt{2}$):

$$\mathrm{Nu} = \left[0.825 + \frac{0.387\,(\mathrm{Ra_H})^{1/6}}{\left[1 + (0.492/\mathrm{Pr})^{9/16}\right]^{8/27}}\right]^2 \tag{11}$$

The total heat flux density transferred by convection and radiation between the inner wall surface and the interior of the passive house is given by [37] as follows:

$$\Phi_i = h_i(T_{wi} - T_i) \tag{12}$$

$$h_i = h_{ri} + h_{ci}, \tag{13}$$

where h_{ri} and h_{ci} are the radiation heat transfer and convective heat transfer coefficients, respectively, on the inside surface of the wall. These coefficients are calculated as follows:

$$h_{ri} = \sigma\varepsilon_w(T_{wi}^2 + T_i^2)(T_{wi} + T_i) \tag{14}$$

$$h_{ci} = \frac{\mathrm{Nu}\lambda_{air}}{H} \tag{15}$$

In order to calculate the Nusselt number, we use the following vertical plate correlations [36]:

$$\mathrm{Nu_H} = 0.516\ \mathrm{Ra_H^{1/4}}\ \text{for}\ 10^4 < \mathrm{Ra_H} < 10^9 \tag{16}$$

$$\mathrm{Nu_H} = 0.117\,\mathrm{Ra_H}^{1/3} \text{ for } 10^9 < \mathrm{Ra_H} < 10^{13} \tag{17}$$

where $\mathrm{Ra_H}$ is the Rayleigh number given by the following:

$$\mathrm{Ra_H} = \frac{g\beta\left(T_{\mathrm{wi}} - T_{\mathrm{i}}\right)H^3}{a\nu} \tag{18}$$

In this study, the solar thermal efficiency of the passive house system is defined as the ratio of the energy absorbed by the air cavity to the total solar energy input [40]:

$$\eta = \frac{Q_{\mathrm{conv}}}{G} \tag{19}$$

Numerical simulation procedure

A numerical simulation of flow and heat transfer in the passive house has been performed using the CFD Fluent code. A two-dimensional steady-state model was used to solve the continuity, momentum and energy equations of air in the domain using the finite volume method. The boundary conditions are specified using the experimental data of a semi-arid typical winter day, for the gap inlet. All walls are considered adiabatic, except the thermal storage wall. The glazing is set as a convective wall boundary, the convective heat transfer coefficient is given by the McAdams expression [37]. The gravitational acceleration was imposed on the air flow. The buoyancy effect was considered using the Boussinesq model. The SIMPLE algorithm was used for the resolution of the velocity–pressure coupling. The characteristics materials constituting the CFD study of passive heating system are summarized in Table 1. The temperature-dependent physical properties of air are given by [39] as follows:

Table 1 Characteristics materials used in the CFD study

Material	Density ρ kg/m^3	Specific heat Cp j/kg k	Conductivity λ W/m °C
Glazing	2500	800	0.8
Adobe	1700	1700	0.6

$$\rho_{\mathrm{air}} = 1.1614 - 0.00353\,(T - 300) \tag{20}$$

$$Cp_{\mathrm{air}} = [1.007 + 0.00004\,(T - 300)] \times 10^3 \tag{21}$$

$$\mu_{\mathrm{air}} = [1.846 + 0.00472\,(T - 300)] \times 10^{-5} \tag{22}$$

$$\lambda_{\mathrm{air}} = 0.0263 + 0.000074\ (T - 300) \tag{23}$$

The relative error between simulation and experimental results is calculated by [41] as follows:

$$\mathrm{Er} = \left|\frac{X_{\mathrm{exp}} - X_{\mathrm{sim}}}{X_{\mathrm{exp}}}\right| \times 100\,\%, \tag{24}$$

where X_{exp} is the experimental value and X_{sim} is the simulation value.

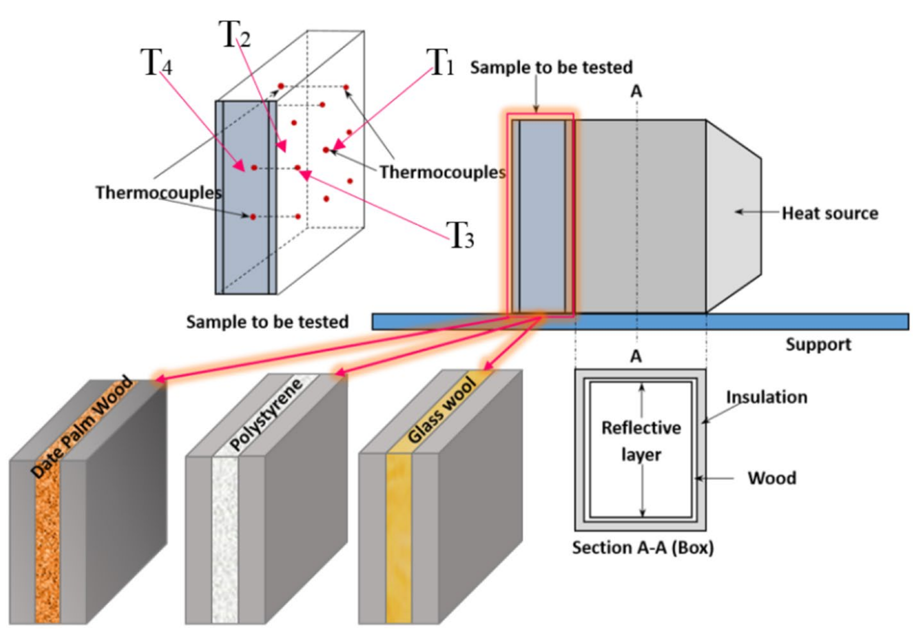

Fig. 7 Test set-up used to obtain the thermal performances of the bio-based material

Results and discussions

Experimental results

In order to evaluate the thermal performances of the bio-based material used for thermal insulation of the passive house prototype, test set-up was carried out, in a previous study, to compare this material to glass wool and expanded polystyrene which are commonly used in building insulation. In the test set-up (Fig. 7), a multilayer wall, formed of the material to be tested between two layers of plasterboard, has been exposed to a constant heat flux. Temperatures are recorded until thermal equilibrium is reached. The physical properties of the tested materials are summarized in Table 2.

For temperature measurements, K type thermocouples were used and connected to a "Testo 176 T4" data logger which transforms the results to a computer for storage and processing. Thermocouples' calibration was performed by an infrared measuring device (Testo 830 type) ensuring rapid and non-contact measurements of the surface temperature. The experiments were carried out under the same conditions and the temperatures are recorded for a period of 1 hour after application of the heat flux, which allows thermal equilibrium to be reached.

The temperature variations of multilayer walls with different insulating materials are shown in Fig. 8. The same tendency is observed for the three materials. We can notice that the bio-based material has the same thermal behavior

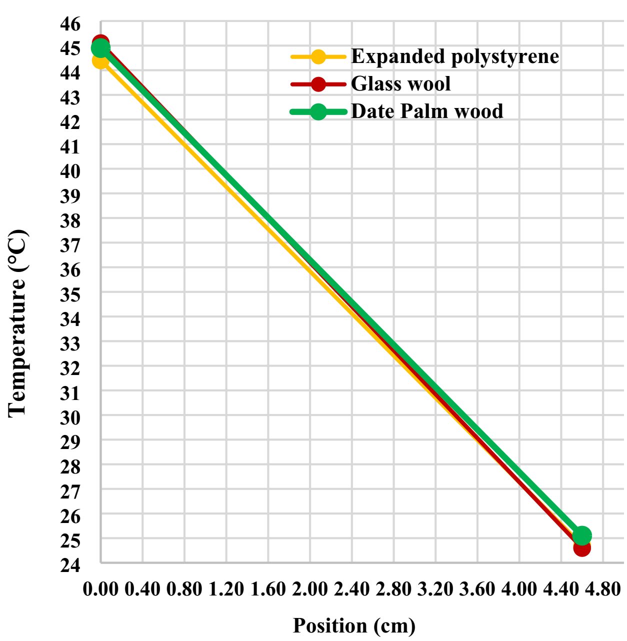

Fig. 8 Temperature variations in multilayer walls for different materials

and thermal insulation capabilities as polystyrene and glass wool. Consequently, the physical properties of date palm wood are close to those of insulation materials commonly used in buildings. The new local bio-based material made from date palm trunks is then used for the insulation of the passive house prototype. The following results were obtained for this passive house prototype. Figures 9 and 10 show indoor air temperature, outdoor air temperature, air gap temperature, solar radiation, relative humidity and wind speed. These data are given for different orientations and for typical winter days, for adobe and stone walls, respectively. The average temperatures in the house and the air gap for different orientations corresponding to the adobe and stone facades are also displayed in Table 3. The maximum temperature difference between the air gap and the interior of the house is obtained for the '160° southeast' orientation. Therefore, '160° southeast' is the optimal orientation for the semi-arid region of Batna.

On the other hand, the large temperature difference is obtained for the adobe storage wall. Consequently, the amount of heat transferred to the house is better for the adobe wall (Table 3).

The air flow rate in the gap during the studied periods is presented in Fig. 11. It can be seen that the largest value of the air flow rate is obtained for the adobe wall corresponding to the optimum orientation (ie. 160° southeast). Heat transfer in the air gap is assumed to be by natural convection between two parallel vertical plates (i.e. the massive wall and the glazing). Average heat transfer coefficients in the air-gap (h_{cc}) and between the outer face of the glass and the ambient outside air (h_{ce}) are shown in Fig. 12. The heat transfer coefficient between the glazing and the outside is due to the wind speed. However, (h_{ce}) is always much higher than (h_{cc}). It can be noticed that the adobe wall is more sensitive to the variation of solar radiation than the stone wall. On the other hand, the average heat transfer coefficient for the stone wall is more important than that of the adobe wall.

Solar heat flux absorbed by the glazing and the Trombe wall at 160° Southeast orientation, for the adobe and stone walls, is presented in Fig. 13. The difference between the two curves represents the losses of the absorbed heat flux between the glazing and the Trombe wall. We can observe the same daily evolution of heat losses between the glazing and the massive wall for both materials (Adobe and stone), except at the end of the day where thermal losses reach the minimum values for Adobe wall compared to the stone wall. This shows that the stone facade has a greater capacity and more time to store heat than the adobe facade.

Solar thermal efficiency is related to the Trombe wall material as illustrated in Fig. 14a. Indeed, the thermal efficiency of the prototype of the passive solar house with an adobe wall is significantly higher than that with a stone wall. Solar thermal efficiency reaches a maximum of 50%

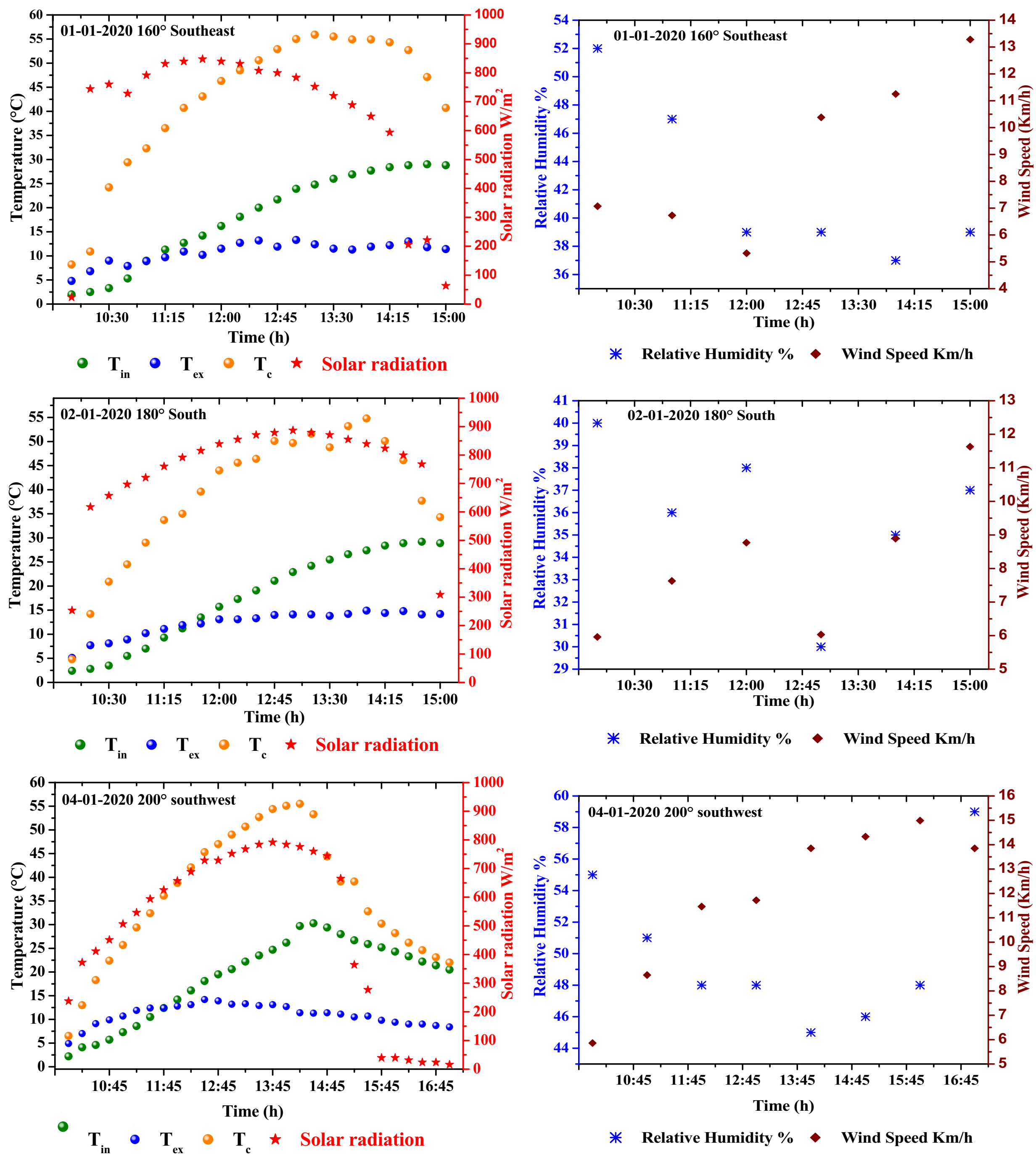

Fig. 9 Temperatures, solar radiation, relative humidity and wind speed for various orientations and for the adobe facade wall

for the adobe wall while it reaches a maximum of 30.7% for the stone wall that is caused by the temperature gradient between the air gap channel and the interior of the house for the adobe wall which is larger than that for the stone wall (Fig. 14b).

Numerical results

A CFD simulation was performed to validate the experimental results. For that purpose, a numerical study on a two-dimensional configuration of the prototype of the passive solar house was carried out using fluid code. The objective of validation is necessary for more reliability and for a better understanding of the air natural convection as well

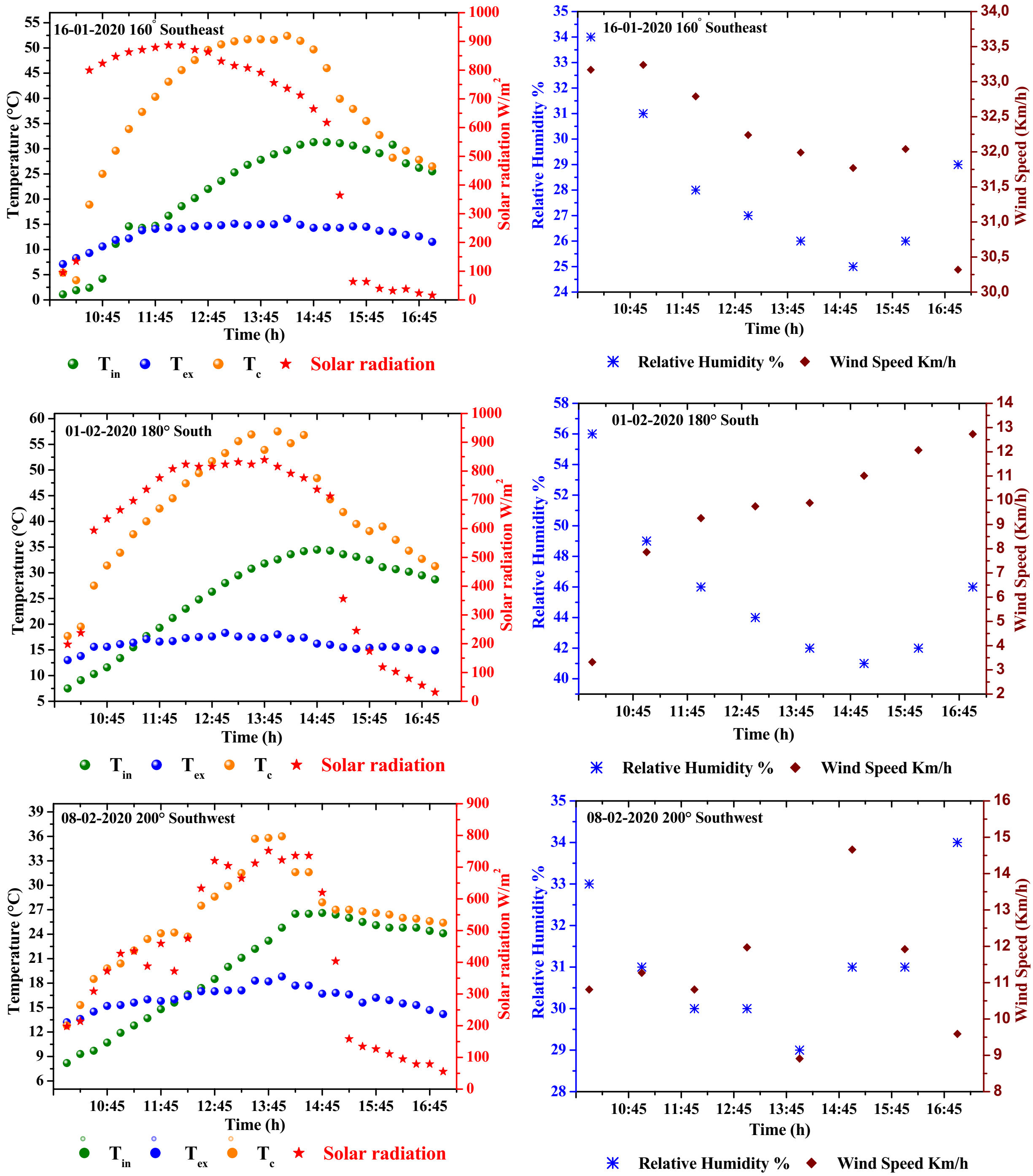

Fig. 10 Temperatures, solar radiation, relative humidity and wind speed for various orientations and for the stone facade wall

as the heat transfer by conduction in the house. Numerical temperature and velocity fields are shown in Figs. 15 and 16, respectively. Two different times of this winter day were chosen to highlight the heat transfer and air velocity of the passive solar heating process, in the morning (at the beginning of the heating process) and in the afternoon (peak or saturation phase) to show the thermal behavior of the passive house and validate the model at these times. After an hour and half of passive heating, at 11:30 the temperature gradient reached the minimum. So the storage wall temperature is at the same temperature as the indoor space. Which means that there will be no reverse air flow in the channel between the outside and the air canal. As a result, the storage wall begins to heat the indoor ambient air. The warm air enters

Table 2 Physical properties of the tested materials

	Density (kg/m^3)	Thermal conductivity (W/m^2 °C)	Specific heat (J/kg °C)
Plasterboard	875	0.21	936
Expanded polystyrene	20	0.042	1404
Glass wool	17	0.035	1030

the room via the top vent driven by the buoyancy force. The air closer to the roof heats up earlier than the lower part, which gradually increases the interior temperature, as shown in Fig. 15a. In the afternoon, at 14:00, the mean air flow velocity in the channel reaches 0.2 m/s (Fig. 16b). Natural convection becomes the dominant heating mode for this period (Fig. 15b). The results are obtained for the adobe wall. A sufficient thermal comfort conditions, with minimal temperature and velocity change in the house are obtained at 14H00.

Table 3 Average internal and air gap temperatures for different orientations

Orientation	160° Southeast			180° South			200° Southwest		
Solar radiation W/m^2	T_i [°C]	T_c [°C]	$\Delta T = T_c - T_i$	T_i [°C]	T_c [°C]	$\Delta T = T_c - T_i$	T_i [°C]	T_c [°C]	$\Delta T = T_c - T_i$
Adobe facade									
650–720	12.6	39.7	27.1	11.3	36.2	24.9	10.6	32.4	21.8
720–800	25.8	55.2	29.4	25.3	51.6	26.3	23.4	52.3	28.9
Stones facade									
650–720	14.2	36.8	22.6	17.4	30.5	13.1	13.4	22.8	9.4
720–800	26.4	51.4	25	39.6	55.4	15.8	22.2	49.7	27.5

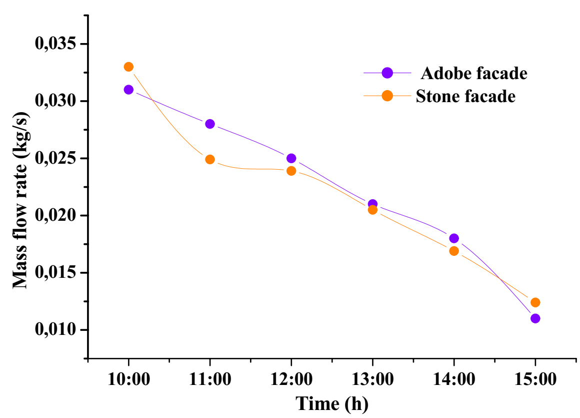

Fig. 11 Air mass flow rate in the air gap channel at 160° Southeast orientation for stone and adobe walls

The experimental and numerical simulation results are in a fair agreement. Indeed, for the internal temperature a relative error of 2.11% and 6.49% was obtained at 11:30 and 14:00, respectively. For solar thermal efficiency, the relative error reaches a maximum of 2.23% and 1.20% at 11:30 and 14:00, respectively (Table 4).

Conclusion

In this work, a passive solar house prototype using Trombe wall system was built and tested in the semi-arid region of Batna, in eastern Algeria. The use of new local bio-insulator

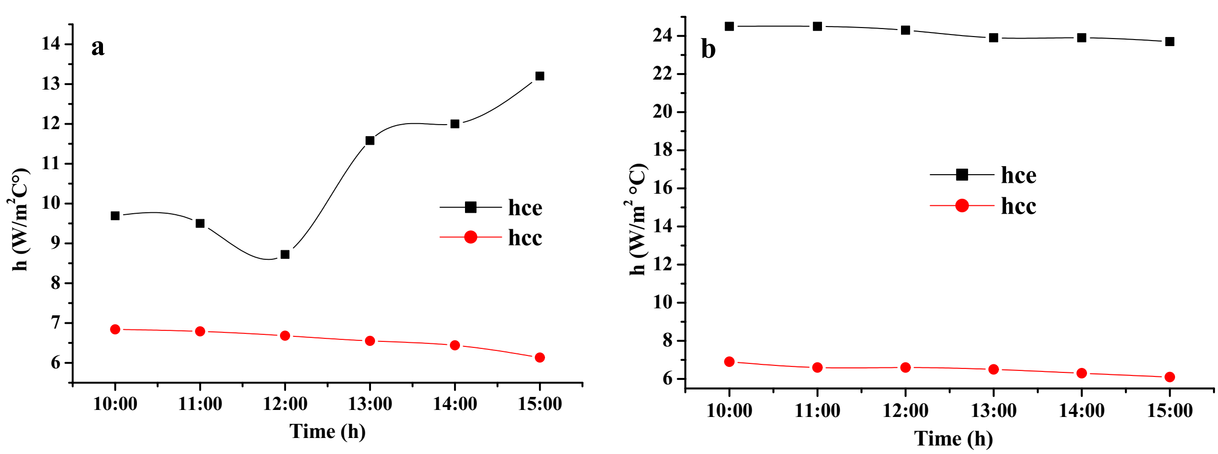

Fig. 12 Average convective heat transfer coefficients at 160° Southeast orientation for **a** adobe wall, **b** stone wall

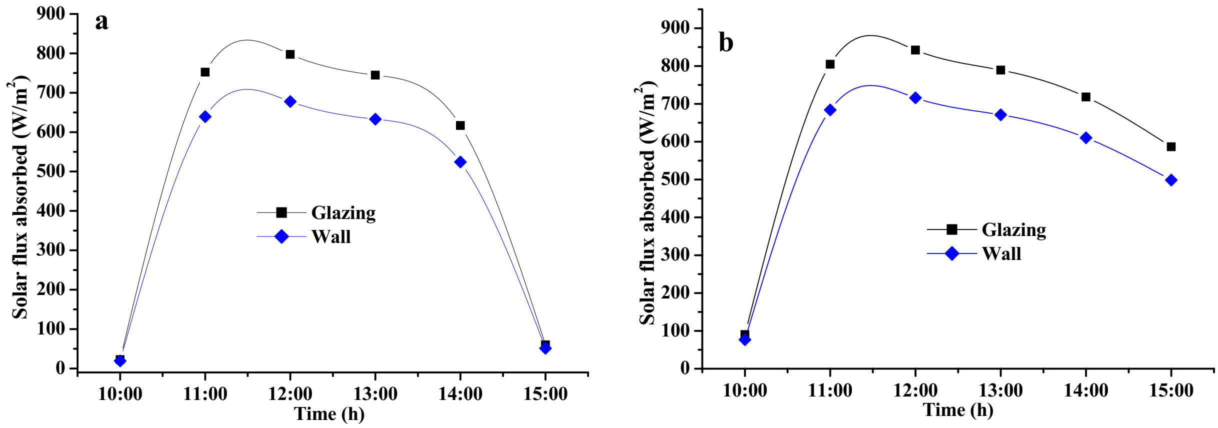

Fig. 13 Solar flux heat absorbed by the glazing and the Trombe wall at 160° Southeast for **a** adobe facade, **b** stone facade

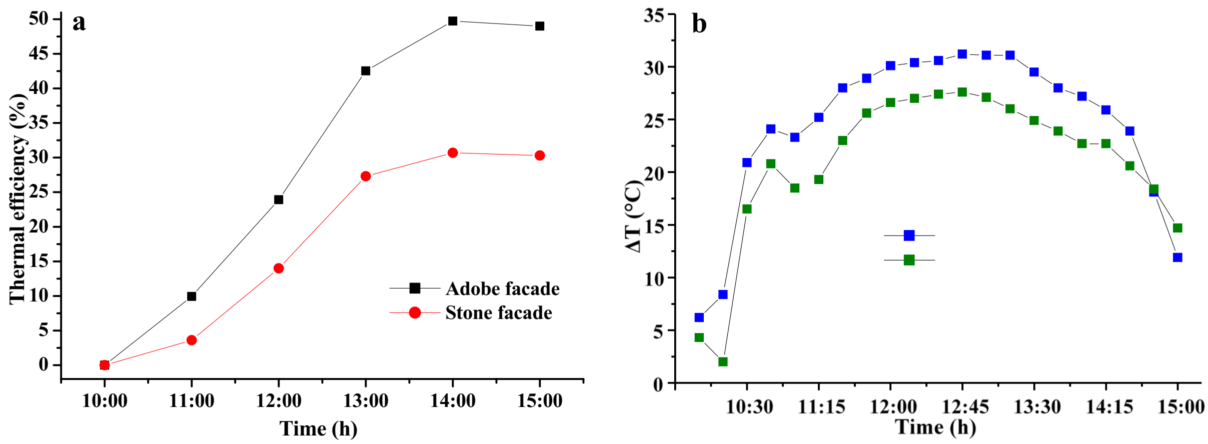

Fig. 14 **a** Solar thermal efficiency for adobe and stone wall at 160° Southeast, **b** Temperature difference between the air gap channel and the interior of the house

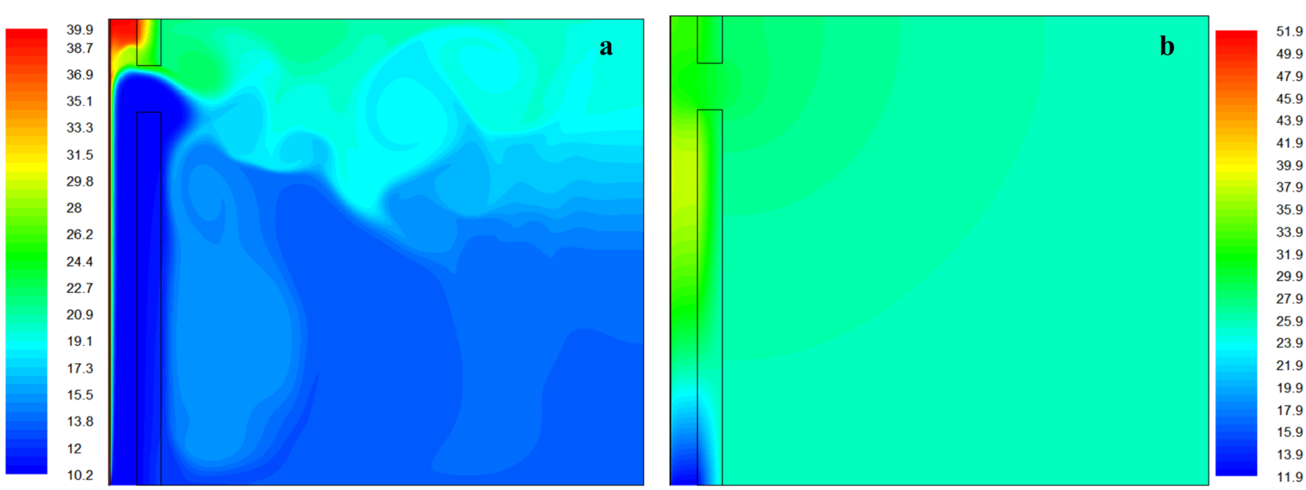

Fig. 15 Temperature contours in the passive house prototype at **a** 11:30, **b** 14:00

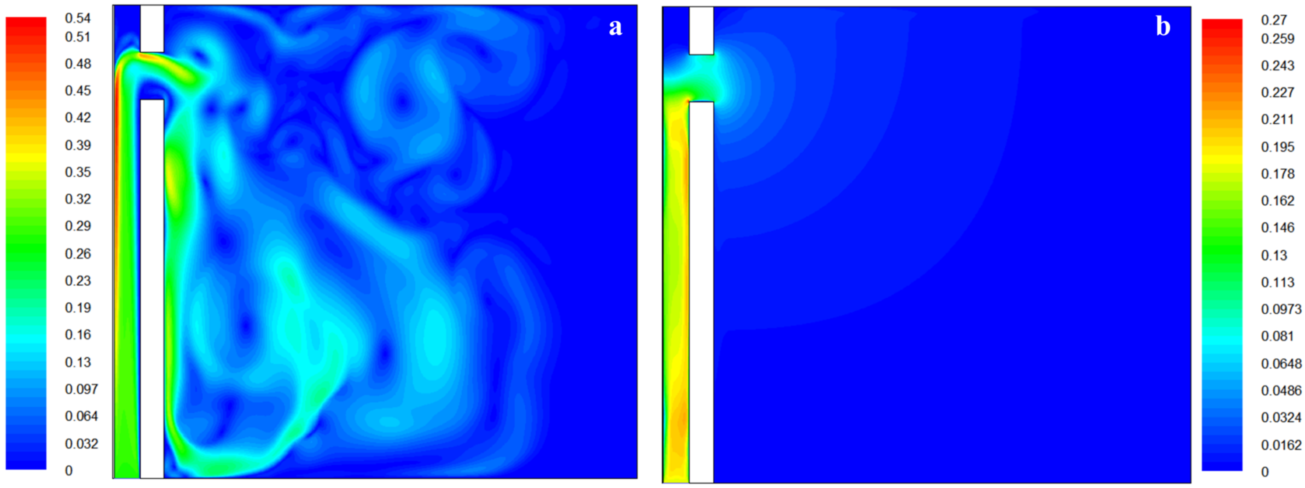

Fig. 16 Velocity contours in the passive house prototype at **a** 11:30, **b** 14:00

Table 4 Relative errors between experimental and numerical simulation results

	Time (h)	
	11:30	14:00
Internal temperature (°C)		
Experimental temperature	14.2	27.7
Numerical simulation temperature	13.9	25.9
Relative error %	2.11	6.49
Solar thermal efficiency (%)		
Experimental efficiency	22.4	49.7
Numerical simulation efficiency	21.9	49.1
Relative error %	2.23	1.20

and bio-based construction materials were discussed. The experimental results show that the Trombe wall thermal behavior is influenced by the nature of the building materials. Indeed, the thermal efficiency of the passive solar house prototype with an adobe wall was found higher than that with a stone wall. A bio-based material made from the trunks of date palms has been used for thermal insulation of the passive house. The physical properties of this bio-based material was found close to those of insulation materials commonly used in buildings. The main results of this research are summarized as follows:

1- The maximum temperature difference between the air gap and the interior of the house is obtained for the '160° southeast' orientation. Therefore, '160° southeast' is the optimal orientation for the semi-arid region of Batna.
2- The amount of heat transferred to the house and the largest value of the air flow rate are better for the adobe wall. On the other hand, the adobe wall is more sensitive to the variation of solar radiation than the stone wall.
3- The same thermal losses were observed between the glazing and the Trombe wall except at the end of the day, for which the thermal losses are minimal for the adobe wall.
4- The daily heat gain from solar energy through the Trombe wall was found to be between 11 and 31% for the stone facade, and between 30 and 50% for the adobe facade.
5- Two-dimensional CFD of passive solar heating system using fluent software has provided a perfect understanding of air circulation by natural convection as well as heat transfer by conduction. The numerical results are in a fair agreement with the experimental data.

Generally, the passive heating system of Trombe wall has been found to be efficient in providing sufficient thermal comfort, in the real semi-arid conditions However, the passive solar house prototype must be tested the rest of the year and adapted according to the needs and requirements of thermal comfort conditions.

Declarations

Conflict of interest On behalf of all authors, the corresponding author states that there is no conflict of interest.

References

1. Özbalta, T.G., Kartal, S.: Heat gain through Trombe wall using solar energy in a cold region of turkey. Sci. Res. Essays **5**, 2768–2778 (2010)
2. Akbarzadeh, A., Charters, W.W.S., Lesslie, D.A.: Thermocirculation characteristics of a Trombe wall passive test cell. Sol. Energy **28**, 461–468 (1982). https://doi.org/10.1016/0038-092X(82)90317-6
3. Bhandari, M.S., Bansal, N.K.: Solar heat gain factors and heat loss. Sol. Energy **53**, 199–208 (1994)
4. Hu, Z., He, W., Ji, J., Zhang, S.: A review on the application of Trombe wall system in buildings. Renew. Sustain. Energy Rev. **70**, 976–987 (2017). https://doi.org/10.1016/j.rser.2016.12.003
5. Liu, Y., Wang, D., Ma, C., Liu, J.: A numerical and experimental analysis of the air vent management and heat storage characteristics of a trombe wall. Sol. Energy **91**, 1–10 (2013). https://doi.org/10.1016/j.solener.2013.01.016
6. Briga Sá, A., Boaventura-Cunha, J., Lanzinha, J.C., Paiva, A.: An experimental analysis of the Trombe wall temperature fluctuations for high range climate conditions: Influence of ventilation openings and shading devices. Energy Build. **138**, 546–558 (2017). https://doi.org/10.1016/j.enbuild.2016.12.085
7. Bajc, T., Todorović, M.N., Svorcan, J.: CFD analyses for passive house with Trombe wall and impact to energy demand. Energy Build. **98**, 39–44 (2015). https://doi.org/10.1016/j.enbuild.2014.11.018
8. Dong, J., et al.: Experimental investigation on the heating performance of a novel designed Trombe wall. Energy (2018). https://doi.org/10.1016/j.energy.2018.11.125
9 Hami, K., Draoui, B., Hami, O.: The thermal performances of a solar wall. Energy **39**, 11–16 (2012). https://doi.org/10.1016/j.energy.2011.10.017
10. Rabani, M., Kalantar, V., Dehghan, A.A., Faghih, A.K.: Experimental study of the heating performance of a Trombe wall with a new design. Sol. Energy **118**, 359–374 (2015). https://doi.org/10.1016/j.solener.2015.06.002
11 Imessad, K., Messaoudene, N.A., Belhamel, M.: Performances of the Barra—Costantini passive heating system under Algerian climate conditions. Renew. Energy **29**, 357–367 (2004). https://doi.org/10.1016/S0960-1481(03)00255-6
12. Jaber, S., Ajib, S.: Optimum design of Trombe wall system in mediterranean region. Sol. Energy **85**, 1891–1898 (2011). https://doi.org/10.1016/j.solener.2011.04.025
13. Abbassi, F., Dimassi, N., Dehmani, L.: Energetic study of a Trombe wall system under different Tunisian building configurations. Energy Build. **80**, 302–308 (2014). https://doi.org/10.1016/j.enbuild.2014.05.036
14. Abdeen, A., et al.: Experimental, analytical, and numerical investigation into the feasibility of integrating a passive Trombe wall into a single room. Appl. Therm. Eng. **154**, 751–768 (2019). https://doi.org/10.1016/j.applthermaleng.2019.03.090
15. Rabani, M., Kalantar, V., Faghih, A.K., Rabani, M., Rabani, R.: Numerical simulation of a Trombe wall to predict the energy storage rate and time duration of room heating during the non-sunny periods. Heat Mass Transfer **49**, 1395–1404 (2013). https://doi.org/10.1007/s00231-013-1175-2
16. Rabani, M., Kalantar, V.: Numerical investigation of the heating performance of normal and new designed Trombe wall. Heat Mass Transfer **52**, 1139–1151 (2016). https://doi.org/10.1007/s00231-015-1616-1
17 Mohamad, A., Taler, J., Ocłoń, P.: Trombe wall utilization for cold and hot climate conditions. Energies **12**, 285 (2019). https://doi.org/10.3390/en12020285
18. Hassanain, A.A., Hokam, E.M., Mallick, T.K.: Effect of solar storage wall on the passive solar heating constructions. Energy Build. **43**, 737–747 (2011). https://doi.org/10.1016/j.enbuild.2010.11.020
19. Bellos, E., Tzivanidis, C., Zisopoulou, E., Mitsopoulos, G., Antonopoulos, K.A.: An innovative Trombe wall as a passive heating system for a building in Athens—a comparison with the conventional Trombe wall and the insulated wall. Energy Build. (2016). https://doi.org/10.1016/j.enbuild.2016.10.035
20. Bevilacqua, P., Benevento, F., Bruno, R., Arcuri, N.: Are Trombe walls suitable passive systems for the reduction of the yearly building energy requirements? Energy **185**, 554–566 (2019). https://doi.org/10.1016/j.energy.2019.07.003
21. Błotny, J., Nemś, M.: Analysis of the impact of the construction of a trombe wall on the thermal comfort in a building located in Wroclaw, Poland. Atmosphere **10**, 761 (2019). https://doi.org/10.3390/ATMOS10120761
22 Szyszka, J., Bevilacqua, P., Bruno, R.: An innovative trombe wall for winter use: the thermo-diode trombe wall. Energies **13**, 2188 (2020). https://doi.org/10.3390/en13092188
23. Jelle, B.P.: Traditional, state-of-the-art and future thermal building insulation materials and solutions—Properties, requirements and possibilities. Energy Build. **43**, 2549–2563 (2011). https://doi.org/10.1016/j.enbuild.2011.05.015
24. Kalnæs, S.E., Jelle, B.P.: Vacuum insulation panel products: a state-of-the-art review and future research pathways. Appl. Energy **116**, 355–375 (2014). https://doi.org/10.1016/j.apenergy.2013.11.032
25. APRUE. Programme de développement de l'éfficacité énergétique à l'horizon 2030. 959, 3267–3271 (2015). http://www.aprue.org.dz/documents/prog.develp.energ-2030.pdf. Accessed 22 Mar 2020
26. Hacène, M.A.B., Sari, N.E.C., Benyoucef, B.: La construction écologique en Algérie: question de choix ou de Moyens ? J. Renew. Energies **14**, 627–635 (2011)
27. Asdrubali, F., D'Alessandro, F., Schiavoni, S.: A review of unconventional sustainable building insulation materials. Sustain. Mater. Technol. **4**, 1–17 (2015). https://doi.org/10.1016/j.susmat.2015.05.002
28. Zach, J., Hroudová, J., Brožovský, J., Krejza, Z., Gailius, A.: Development of thermal insulating materials on natural base for thermal insulation systems. Procedia Eng. **57**, 1288–1294 (2013). https://doi.org/10.1016/j.proeng.2013.04.162
29 Amziane, S., Sonebi, M.: Overview on bio-based building material made with plant aggregate. RILEM Tech. Lett. **1**, 31–38 (2016)
30. Belaid, D.: La culture du palmier dattier en Algérie. Collection : Sciece et techniques agronomique. pp 197 (2015). http://www.djamel-belaid.fr/app/download/24526734/LivrePalmier.pdf. Accessed 16 Sep 2019
31. Srivaro, S., Chaowana, P., Matan, N., and Kyokong,B. : Lightweight sandwich panel from oil palm wood core and rubberwood veneer face. Journal of Tropical Forest. 26, 50–57 (2014). https://www.jstor.org/stable/23617013. Accessed 16 Sep 2019
32. Haseli, M., Layeghi, M., Hosseinabadi, H.Z.: Characterization of blockboard and battenboard sandwich panels from abstract.

Measurement (2018). https://doi.org/10.1016/j.measurement.2018.04.040
33. Boumhaout, M., Boukhattem, L., Hamdi, H., Benhamou, B.: Thermomechanical characterization of a bio-composite building material : Mortar reinforced with date palm fibers mesh. Constr. Build. Mater. **135**, 241–250 (2017). https://doi.org/10.1016/j.conbuildmat.2016.12.217
34. Amara, I., Mazioud, A., Boulaoued, I., Mhimid, A.: Experimental study on thermal properties of bio-composite (gypsum plaster reinforced with palm tree fibers) for building insulation. Int. J. Heat Technol. **35**, 576–584 (2017). https://doi.org/10.18280/ijht.350314
35. Ghofrani, M., Ashori, A., Mehrabi, R.: Mechanical and acoustical properties of particleboards made with date palm branches and vermiculite. Polym. Testing **60**, 153–159 (2017). https://doi.org/10.1016/j.polymertesting.2017.03.028
36. Rabani, M., Kalantar, V., Rabani, M.: Heat transfer analysis of a Trombe wall with a projecting channel design. Energy **134**, 943–950 (2017). https://doi.org/10.1016/j.energy.2017.06.066
37. Dimassi, N., Dehmani, L.: Experimental heat flux analysis of a solar wall design in Tunisia. J. Build. Eng. (2016). https://doi.org/10.1016/j.jobe.2016.10.001
38. Shen, J., Lassue, S., Zalewski, L., Huang, D.: Numerical study of classical and composite solar walls by TRNSYS. J. Therm. Sci. **16**, 46–55 (2007). https://doi.org/10.1007/s11630-007-0046-x
39. Dragićević, S., Lambic, M.: Influence of constructive and operating parameters on a modified Trombe wall efficiency. Arch. Civi Mech. Eng. **11**, 825–838 (2011). https://doi.org/10.1016/s1644-9665(12)60080-6
40. Lewandowski, W.M., Lewandowska-Iwaniak, W.: The external walls of a passive building: a classification and description of their thermal and optical properties. Energy Build. **69**, 93–102 (2014). https://doi.org/10.1016/j.enbuild.2013.10.021
41. Hong, X., He, W., Hu, Z., Wang, C., Ji, J.: Three-dimensional simulation on the thermal performance of a novel Trombe wall with venetian blind structure. Energy Build. **89**, 32–38 (2015). https://doi.org/10.1016/j.enbuild.2014.12.014